UMERC+METS
2024 Conference

7-9 August | Duluth, MN, USA

Introduction of a Full Bridge Converter with Maximum Power Point Tracking Control for Efficient Tidal Energy Harvesting

Emma Geon[a1], Roshan Kini[a2], Linnea Weicht[a3], Benjamin Roberts[a1], Alex Turpin[a1]

[a1]*Pacific Northwest National Laboratory (PNNL) – Sequim 1529 W Sequim Bay Rd, Sequim, WA 98382*
[a2]PNNL - *Richland 902 Battelle Blvd, Richland, WA 99354*
[a3]*PNNL – Seattle 1100 Dexter Ave N, Seattle WA 98109*

Abstract

Marine renewable energy provides a potentially vast power source which can be harnessed for sustainable energy in areas at sea and along the coast. Tidal energy specifically is characterized by strong predictability and consistent availability. However, energy harvesting systems such as tidal turbines currently lack efficient and affordable power conversion systems that can handle the high peak to average power ratios associated with tidal energy. We present a tidal power converter topology with maximum power point tracking control for use in this application. The converter is discussed with respect to existing solutions and tested in a MATLAB-Simulink model to demonstrate its novelty.

Keywords: tidal energy; hardware-in-the-loop; full-bridge converter; maximum power point tracking; perturb and observe algorithm;

1. Introduction

Marine energy (ME), derived from ocean waves and tidal currents, presents a carbon-free, sustainable power source which is particularly beneficial in remote areas with limited access to energy. Several applications, such as power for ocean observing buoys or small autonomous surface vehicle (ASV) recharging, offer an immediate opportunity for MRE to demonstrate feasibility. These applications often have small-scale (<1kW) power requirements [1] and necessitate high system efficiency to be competitive with alternate renewable sources of power to overcome the cost of installation. However, tidal energy is often characterized by high peak power output and low mean power, which is a challenge for efficient power systems. To succeed in wider ranges of voltages and power in tidal energy generation, robust power electronics and precise control must be able to maintain efficiency while handling high peak to mean power output.

In an effort to identify existing off the shelf power electronics for use with tidal turbines, this team found several components such as a solar charge controller from MidNite Solar [2], and an e-bike motor controller from Grin Technologies [3]. However, each of these components required modification to be compatible with tidal turbine power profiles and control schemes. Even with modifications, these solutions are not ideal. Hurdles remain, such as the solar charge controller's tendency to enter "resting" mode as incoming voltage stagnates. Other marine energy researchers, such as those at the University of New Hampshire, have used industrial motor controllers in a regenerative application

for tidal turbines (R. Cavagnaro, personal communication, October 15, 2024). This approach controls turbine operating point, but such designs do not prioritize the efficiency of mechanical to electrical power conversion, and they consider only turbines with three-phase grid connection. Currently, findings of our literature review and market analysis indicate that tidal energy lacks a commercial off-the-shelf (COTS) option for handling wide ranges of power conversion efficiently, particularly for off-grid applications.

This work presents the design of a full bridge-based power converter which considers the high peak to average power output expected from a tidal turbine. The converter is a combination of a passive rectifier with a full bridge DC to DC converter accepting a wide range of input voltages. It is implemented with a maximum power point tracking (MPPT) control strategy and evaluated using a MATLAB-Simulink model. Additional existing solutions in this space and their limitations are discussed, as is the potential for this power converter.

2. Methods

2.1. Power Converter Topology

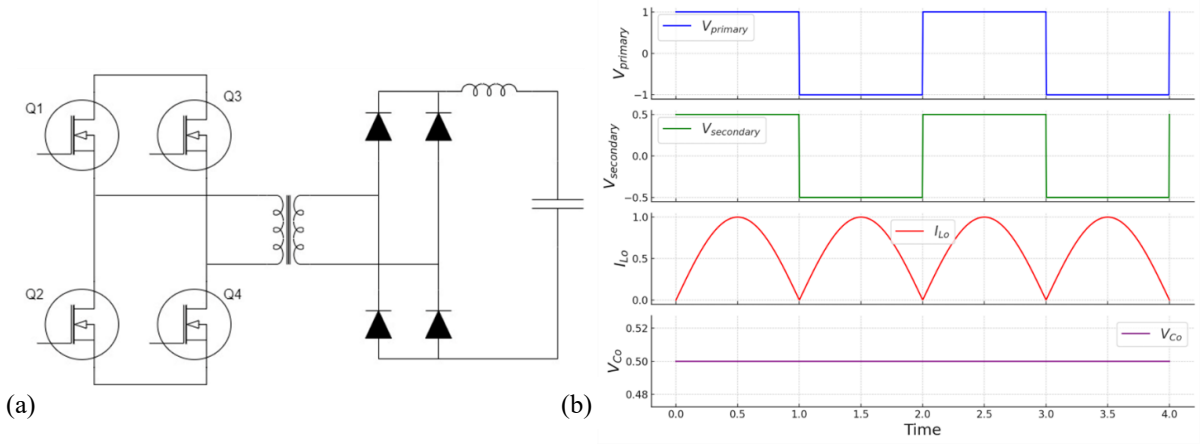

Figure 1: Full bridge converter (a) topology (b) switching waveforms including the primary voltage alternating between positive and negative source voltage, and the secondary voltage scaled by the turns ratio, the output inductor current (I_{Lo}) displaying characteristic ripple, and the output capacitor voltage (V_{co}) maintaining a relatively constant value with minor ripple.

A full bridge DC-DC converter is implemented using four switches arranged in an H-bridge configuration, which is connected to a high-frequency switching transformer as shown in Figure 1a. The H-bridge operates by alternately switching the transistors on and off, creating a high-frequency AC voltage across the primary winding of the transformer. This AC voltage is then either stepped up or stepped down by the transformer, depending on the required output magnitude, and subsequently rectified and filtered to produce a stable DC output voltage. The operation of a full bridge converter involves different switching modes, typically characterized by the states of the four switches. In each switching cycle, two switches on opposite sides of the bridge are turned on simultaneously, creating a path for current to flow through the primary winding of the transformer. This alternation between the two pairs of switches results in a square wave voltage across the transformer as shown in Figure 1b. On the secondary side, the primary-side voltage is adjusted according to the turns ratio, then rectified and filtered to produce a stable DC output voltage. This output voltage is regulated by adjusting the duty cycle or the phase shift of the PWM signal controlling the switches.

To design a suitable full-bridge converter, it is essential to determine the appropriate turns ratio and properly design the output filter capacitor and inductor. This ensures the minimization of RMS voltage and RMS current across the output capacitor (Co) and the output inductor (Lo), respectively. The formula for determining turns ratio (N_p/N_s) is calculated using (1), where V_o represents the output voltage, V_s represents the input/source voltage, N_p is primary turns, and N_s is secondary turns. Additionally, D is the duty cycle. The formulas for calculating minimum output inductor and capacitor are presented in (2) and (3) where ΔI_{LO} is the output ripple current and ΔV_{peak} is the maximum peak-to-peak voltage ripple.

$$D = \left(\frac{V_o}{2 * V_s}\right) * \frac{N_p}{N_s} \quad (1)$$

$$Lo \geq \left(\frac{V_o \times (1 - \mathrm{D})}{\Delta I_{LO} \times \mathrm{fs}}\right) \quad (2)$$

$$Co \geq \left(\frac{I_o \times (1 - \mathrm{D})}{\Delta V_{peak} \times \mathrm{fs}}\right) \quad (3)$$

2.2. Control Design

Maximum Power Point Tracking (MPPT) algorithms are commonly used in many renewable energy applications. Due to the variable nature of a natural source, the ability to track and modify the operating point to optimize output over a wide range of input conditions is necessary. Overall, MPPT strategies can be characterized as sensor-based or sensorless [4].

Examples of sensor-based MPPT algorithms include intracycle control which utilizes an encoder to determine the angular position of the crossflow turbine [5] and axial induction factor control which utilizes Acoustic Doppler Current Profilers (ADCP) to measure tidal flow velocity [6]. Another sensor-based method to note is the Kw^2 control algorithm [7]. This method requires measurement of the turbine angular velocity to implement a resistive torque controller with the use of coefficient K. This value is very specific to the turbine at the time tested and can vary over its lifetime as the hydrodynamic profile of the turbine changes through corrosion, biofouling, etc. The addition of sensors into the control of tidal turbines can be valuable but introduces more cost, complexity, and adds a potential point of failure to the system. For these reasons we decided to pursue a sensorless control method for our application.

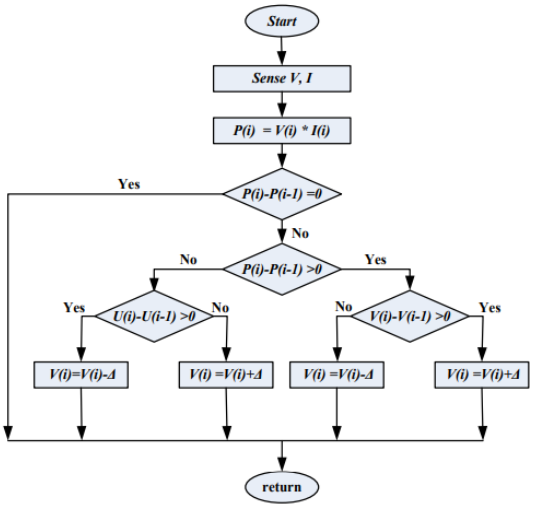

Sensorless MPPT algorithms depend on tracking the power changes of the system and adjusting the operating point according to the specific method being utilized. The most well-known of these methods is the perturb and observe (P&O) algorithm [4]. The P&O algorithm operates by perturbing the operating point of the system through incrementing the input voltage and observing its impact on the subsequent output power [8]. A flowchart depicting this operation is shown in Figure 2. Incrementation of the input voltage is often achieved through varying the duty cycle by a constant value, the goal of which is to find the operating point where the time derivative of power is equal to zero indicating the system is operating at its maximum power point. While this method is most commonly used in Photovoltaic (PV) Systems, it has been implemented into the control of a tidal turbine with promising results [9].

Figure 2: Flowchart of Perturb and Observe Algorithm [6]

The method detailed above is able to implement the P&O algorithm with very little external sensing needed, only having included an encoder into the system. For our control algorithm our goal was to develop a novel P&O controller for tidal applications that utilized no sensors external to the controller electronics. This system would ideally be agnostic to the integrated power source and easily configurable in a wide variety of applications. To accomplish this a highly accurate input voltage and current measurement needs to be integrated into the power electronics system. These measurements will serve to calculate the input power that we are tracking in this algorithm.

The goal of implementing a control method like P&O is to determine and output the maximum power of the system for the given operating conditions. For a cross-flow turbine this is achieved by regulating the Tip Speed Ratio (TSR) to alter the Coefficient of Performance (C_p). TSR is the ratio of the blade tip speed to the speed of incoming tidal velocity and C_p is a characteristic profile specific to the turbine that dictates its efficiency [10]. Without having integrated measurements of these values as input to the control algorithm it is important to understand how these variables are related to load power and turbine operation. As the turbine spins up both the TSR and C_p values increase. Once it is fully spun up TSR will be at its maximum value of around 3 for our simulated turbine. Ideally at this point in operation the electronics system would start pulling power which will cause the turbine to slow, decreasing the TSR value. This increase in power output of the system will also cause the C_p value to increase. These values will continue to trend in their respective directions until they stabilize into their steady state values. For our simulated turbine to be operating in the stable region the TSR must stabilize at a value above 1.8 with a C_p value of around 0.25. This relationship can be visualized below in Figure 3a. The function of the control algorithm is to modulate the power demanded by the electronics system to drive the TSR and C_p to these steady state values.

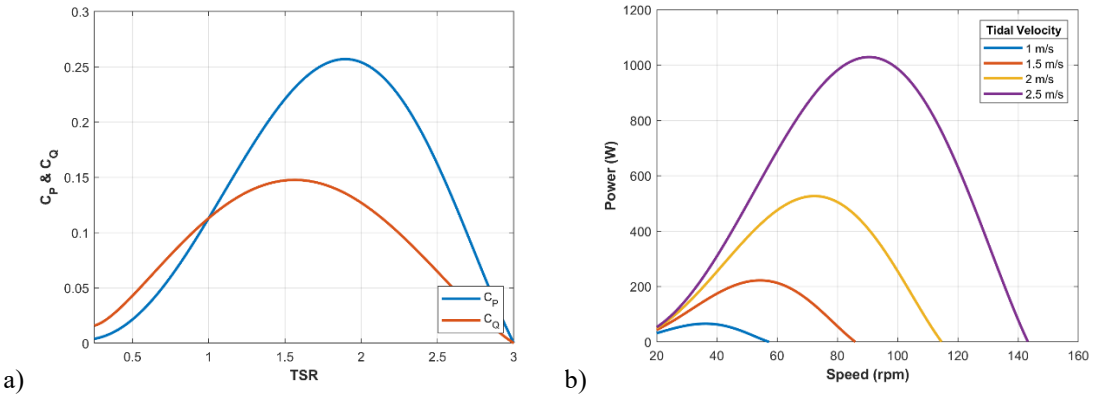

Figure 3: a) Turbine TSR v. Cp and CQ b) Generator Speed v. Turbine Output Power

A turbine with a convex TSR-C_P characteristic, as depicted above in Figure 3, creates some complications in the application of the traditional P&O algorithm. This operation and its subsequent changes to the P&O method can be divided into two parts, turbine spin up and spin down. During the spin up process it is important that the electronics not pull power too early. Inserting a high resistive load into the system before the turbine has fully spun up could cause the turbine to stall out or result in operation in the unstable and inefficient region of turbine performance. To prevent this from happening a condition is added into the initial checks of the P&O algorithm. This function queries the source voltage and will only allow a PWM signal to be sent to the power electronics if the source voltage is over a specified threshold value, which in our case is 55V. Once this threshold value is surpassed the P&O method begins and will start sending PWM signals to the Full Bridge converter. This allows the turbine to spin up freely before the electronics start demanding power.

Once the threshold voltage has been reached, the P&O method will begin by calculating the source power and ideal duty cycle of the Full Bridge converter at its current input conditions using Equation 1. Then it determines the change in both the source power and voltage by subtracting it from its previous value. Once all of these values have been calculated the program will determine if the power is increasing or decreasing and begin with the traditional P&O algorithm. This process ensures that as the power changes, we are tracking the maximum output power as well as holding the TSR and C_p at their ideal values, resulting in stable operation of the turbine.

3. Validation (Simulink):

In order to validate the functionality of the Full Bridge converter and characterize the performance of the P&O control algorithm, a MATLAB Simulink model was developed for testing. A tidal velocity signal is input to the model. This data was produced by PNNL's Finite Volume Coastal Ocean Model-based (FVCOM-based) Salish Sea model [11], [12], refined for a Sequim Bay, WA use case and therefore represents accurate tidal velocities that would be experienced in the field. This tidal speed is then fed into the tidal turbine function which is largely based on previous work conducted to create a LabView based Tidal Turbine Emulator (TTE) [13]. The turbine model uses tidal velocity

to calculate the TSR and C_p values as well as an output turbine torque. This output torque is then multiplied by our gear ratio value to represent the gear box between the turbine and the generator. The output of this calculation is the generator torque which is fed into a predefined permanent magnet synchronous generator model. This generator outputs three-phase AC voltage that is then converted to DC voltage through a passive rectifier. This DC voltage is the input to the Full Bridge converter. The P&O algorithm is implemented via a MATALB function that takes the source voltage and current as input and outputs a duty cycle. This duty cycle is then converted into a PWM signal which is sent to the full bridge converter to modulate its operation. On the output, a 60 V battery is used as the load. Selected simulation and full bridge parameters are detailed in Tables 1 and 2, respectively.

Table 1. Select Simulation Parameters.

Parameter	Value
Turbine Cross-section	0.5 m^2
Turbine Inertia	4.025 $kg\ m^2$
Gear Ratio	1:16
Generator Rated Speed	3750 *RPM*
Generator Rated Voltage	300 *V*
Generator Rated Torque	1.7 *Nm*

Table 2. Select Converter Parameters.

Parameter	Value
Input Voltage Range	30-150 *V*
Capacitor	10 *mF*
Inductor	0.9 *mH*
Turns Ratio	0.167
Rectifier Filter Capacitor	0.5 *mF*

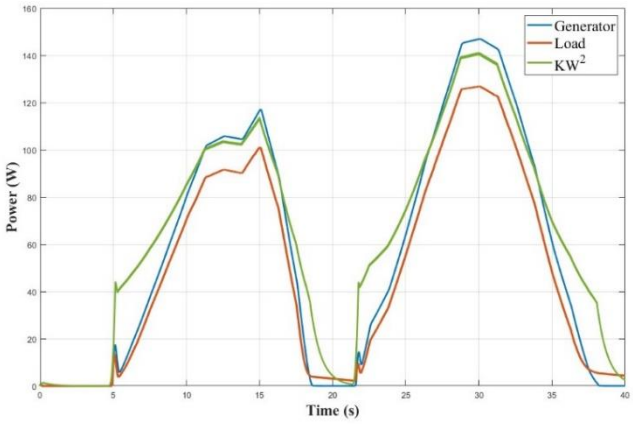

Figure 4. Simulated generator power output (Generator), power measured at the load (Load), and theoretical power based on Kw2 torque (Kw2).

To demonstrate the efficacy of the control methodology, a section of tidal velocity data was chosen that encompasses a full tidal exchange. This tidal profile starts at 0.5 m/s right below the selected cut in speed of 0.6 m/s. The tidal velocity then slowly increases to a peak value of 1.6 m/s before descending and repeating the pattern. Results, shown in Figure 4, indicate the control scheme and converter topology's ability to accurately track MPPT power and harvest energy efficiently. Additionally, the coefficient of performance is able to reach its maximum value of 0.25 for each of the stretches of velocity above cut-in speed.

4. Future Work:

The full bridge converter and MPPT algorithm that have been validated in Simulink modeling will be implemented using PNNL's tidal turbine emulator (TTE) [13]. The TTE is currently being used to test alternative solutions such as a Midnite Solar charge controller programmed for our modeled tidal turbine's power curve. Additional testing will explore the efficiency of our chosen power converter topology and control scheme compared with several off the shelf parts modified for a tidal turbine application and alternate converter designs. Additional optimal control schemes will be explored, and all parts will be tested with more robust simulated turbulence.

Acknowledgements

The authors would like to acknowledge Robert J. Cavagnaro and Andrea Copping for technical and conceptual guidance, respectively.

References

[1] A. E. Copping, R. E. Green, R. J. Cavagnaro, D. S. Jenne, D. M. Greene, J. J. Martinez and Y. Yang, "Powering the Blue Economy - Ocean Observing Use Cases Report," Pacific Northwest National Laboratory, 2020.

[2] MidNite Solar, "Charge Controllers - Classics," [Online]. Available: https://www.midnitesolar.com/productPhoto.php?menuItem=products&productCat_ID=21&product_ID=256. [Accessed 30 9 2024].

[3] Grin Technologies, "Grin Technologies," [Online]. Available: https://ebikes.ca/product-info/grin-products/baserunner.html. [Accessed 1 10 2024].

[4] M. Wen, Y. Ren and N. Srikanth, "Review of Maximum Power Point Tracking Algorithm for Tidal Turbine Generator," *Asian Wave and Tidal Energy Conference,* 2016.

[5] B. Strom, S. Brunton and B. Polagye, "Intracycle Angular Velocity Control of Cross-Flow Turbines," *Nature Energy,* 2017.

[6] Y. Zhang, J. Shek and M. Mueller, "Controller Design for a tidal turbine array, considering both power and load aspects," *Renewable Energy,* 2023.

[7] D. Forbush, R. J. Cavagnaro and B. Polagye, "Power-tracking control for cross-flow turbines," *Renewable and Sustainable Energy,* 2019.

[8] A. M. Eltamaly, "Performance of MPPT Techniques of Photovoltaic Systems Under Normal and Partial Shading Conditions," *Advances in Renewable Energies and Power Technologies,* vol. 1: Solar and Wind Energies, pp. 115-161, 2018.

[9] S.-H. Moon, B.-G. Park, J.-W. Kim and J.-M. Kim, "Maximum Power Point Tracking Control Using Perturb and Observe Algorithm for Tidal Current Generation System," *Precision Engineering and Manufacturing Green Technology,* 2020.

[10] N. Mehmood, Z. Liang and J. Khan, "Diffuser Augmented Horizontal Axis Tidal Current Turbines," *Applied Sciences, Engineering, and Technology,* 2012.

[11] Z. Yang and T. Yang, "Tidal residual eddies and their effect on water exchange in the puget sound," *Ocean Dynamics,* vol. 63, pp. 995-1009, July, 2013.

[12] Z. Yang, T. Wang, A. Copping and S. Geerlofs, "Modeling of in-stream tidal energy development and its potential effects in Tacoma Narrows, Washington, USA," *Ocean & Coastal Managment,* vol. 99, pp. 52-62, October, 2014.

[13] L. Weicht, A. Turpin and B. Roberts, "Hardware-in-the-Loop Efficiency Analysis of Tidal Power Systems," *Pacific Northwest National Lab,* 2023.